





An investigation of effect of different nuclear potentials on CDCC calculations: $^{11}\text{Be} + ^{120}\text{Sn}$ reaction

Şule KARATEPE ÇELİK^{1,*} , Murat AYGÜN² 

¹Bitlis Eren University, Hizan Vocational School, Bitlis/ TURKEY

²Bitlis Eren University, Department of Physics, Bitlis/ TURKEY

Abstract

Aim of this study is to examine the effect of various potentials on continuum discretized coupled channel (CDCC) calculations. For this, the elastic scattering cross section of ^{11}Be projectile from ^{120}Sn target is calculated by using ten different potentials. The results are compared with experimental data.

Article info

History:
Received: 29.04.2020
Accepted: 02.09.2020

Keywords:
Nuclear potential,
proximity potential,
CDCC model,
Optical model

1. Introduction

Nuclear potential plays an important role in explaining nuclear reactions. Although there are different nuclear potentials in the literature, determining alternative potentials is still one of the hot topics of nuclear physics. Proximity potentials have an important place among alternative nuclear potentials, and have widely been evaluated in analysing cluster decay and fusion reactions [1-4]. Recently, proximity potentials have also been applied on elastic and quasielastic scattering reactions [5-8].

Continuum discretized coupled channel (CDCC) is an effective model in explaining different nuclear interactions such as elastic scattering, inelastic scattering, breakup reaction. In this respect, a lot of studies as theoretical and experimental have been performed [9-13]. Theoretical studies have been carried out using different potentials. However, it is still needed to determine new alternative nuclear potential for CDCC calculations.

In this paper, we aim to get alternative potentials in CDCC analysis of nuclear interactions. Our study consists of three steps. In one step, the elastic scattering cross-section (ESCS) of $^{11}\text{Be} + ^{120}\text{Sn}$ system is calculated by using eight type potentials. In the second and third steps, the calculations are performed for

phenomenological and double folding potentials, respectively.

2. Theoretical Formalism

2.1. CDCC model

In this study, we use the CDCC model within the optical model limits to explain $^{11}\text{Be} + ^{120}\text{Sn}$ system, which is evaluated in describing nuclear interactions. In the CDCC model, projectile is considered as nucleon-core system, and total system are composed as nucleon-core, nucleon-target and core-target. Discretization has been obtained by the average method (A_v) in the CDCC calculation [14,15]. In the CDCC calculations, coupled channel equation is

$$[E - K_R - \varepsilon_i]\chi_i(r) = \sum_j^N \langle \phi_i | U | \phi_j \rangle \chi_j(R),$$

where the bound and discretized continuum states are demonstrated by ϕ_i , U is total potential, and ε_i is energy of nucleon-core system [14]. S-matrix elements are obtained with solving this equations.

The projectile ^{11}Be is assumed as $^{11}\text{Be} \rightarrow ^{10}\text{Be} + n$ in the calculations, and is discretized to energy bins. Thus, $^{11}\text{Be} + ^{120}\text{Sn}$ system is evaluated as $n + ^{10}\text{Be}$, $n + ^{120}\text{Sn}$ and $^{10}\text{Be} + ^{120}\text{Sn}$. The nuclear potentials of $n + ^{10}\text{Be}$ and $n + ^{120}\text{Sn}$ systems are taken from Ref. [16] and Ref. [17], respectively. On the other hand, the nuclear potential of $^{10}\text{Be} + ^{120}\text{Sn}$ system is calculated by using

*Corresponding author. e-mail address: skaratepe@beu.edu.tr
<http://dergipark.gov.tr/csj> ©2020 Faculty of Science, Sivas Cumhuriyet University

eight different proximity type potentials, phenomenological potential and double folding potential whose a brief summary is given in the following subsection. The CDCC calculations have been performed by the code FRESKO.

2.2. Potentials

2.2.1. Promimity 1977, 2003-I, 2003-II, 2003-III and 2010 potentials

Proximity 1977 (Prox 77) [18] can be written as

$$V(r) = 4\pi\gamma b\bar{R}\Phi(\xi) \text{ MeV}, \tag{2}$$

where

$$\gamma = \gamma_0 \left[1 - k_s \left(\frac{N-Z}{N+Z} \right)^2 \right], \quad b \approx 1 \text{ fm}, \quad \bar{R} = \frac{c_1 c_2}{c_1 + c_2}, \tag{3}$$

and

$$C_i = R_i \left[1 - \left(\frac{b}{R_i} \right)^2 + \dots \right], \quad R_i = 1.28A_i^{1/3} - 0.76 + 0.8A_i^{-1/3} \text{ fm}, \quad (i = 1,2) \tag{4}$$

with

$$\Phi(\xi) = \begin{cases} -\frac{1}{2}(\xi - 2.54)^2 - 0.0852(\xi - 2.54)^3 & \xi \leq 1.2511, \\ -3.437 \exp\left(-\frac{\xi}{0.75}\right) & \xi \geq 1.2511, \end{cases} \tag{5}$$

Proximity 2003-I, 2003-II, 2003-III and 2010 potentials are same as that of Prox 77, but for different parameters listed in Table 1 [17, 18].

Table 1. Parameters of Prox 77, Prox 2003-I, Prox 2003-II, Prox 2003-III and Prox 2010 potentials.

Potential type	γ_0 , MeV/fm ²	k_s
Prox 77	0.9517	1.7826
Prox 2003-I	1.08948	1.9830
Prox 2003-II	0.9180	0.7546
Prox 2003-III	0.911445	2.2938
Prox 2010	1.460734	4.0

2.2.2. Broglia and Winther 1991 (BW 91) potential

BW 91 potential is defined as [3]

$$V(r) = -\frac{V_0}{\left[1 + \exp\left(\frac{r-R_0}{a}\right) \right]}, \quad V_0 = 16\pi \frac{R_1 R_2}{R_1 + R_2} \gamma a, \quad a=0.63 \text{ fm}, \tag{6}$$

where

$$R_0 = R_1 + R_2 + 0.29, \quad R_i = 1.233A_i^{1/3} - 0.98A_i^{-1/3} \text{ fm} \quad (i = 1,2), \quad \gamma = 0.95 \left[1 - 1.8 \left(\frac{N_1 - Z_1}{A_1} \right) \left(\frac{N_2 - Z_2}{A_2} \right) \right]. \tag{7}$$

2.2.3. Aage Winther (AW 95) potential

AW 95 potential [4,16] is the same as the other parameters of BW 91 potential except for the following parameters

$$a = \frac{1}{1.17(1+0.53(A_1^{-1/3}+A_2^{1/3}))}, \quad R_0 = R_1 + R_2, \quad R_i = 1.2A_i^{1/3} - 0.09 \text{ fm} \quad (i = 1,2). \quad (8)$$

2.2.4. Chirstensen and Winther 1976 (CW 76) potential

CW 76 is [19]

$$V(r) = -50 \frac{R_1 R_2}{R_1 + R_2} \Phi \left(\frac{r - R_1 - R_2}{0.63} \right) \text{ MeV}, \quad (9)$$

$$R_i = 1.233A_i^{1/3} - 0.978A_i^{-1/3} \text{ fm} \quad (i = 1,2). \quad (10)$$

2.2.5. Phenomenological potential

The phenomenological potential is assumed as

$$V_N(r) = - \frac{V_0}{\left[1 + \exp\left(\frac{r - R_V}{a_V}\right)\right]} - i \frac{W_0}{\left[1 + \exp\left(\frac{r - R_W}{a_W}\right)\right]} \quad (11)$$

where V_0 and W_0 are the depths of real and imaginary potentials, $R_{V(W)}$ is the nuclear radius of real(imaginary), and $a_{V(W)}$ is the diffusion parameter of real(imaginary), respectively.

2.2.6. Double folding potential

The double folding potential can be presented as

$$V = \int d\vec{r}_1 \int d\vec{r}_2 \rho_1(r_1) \rho_2(r_2) v_{NN}(r_{12} = |\vec{R} + \vec{r}_2 - \vec{r}_1|) \quad (12)$$

where, $\rho_1(r_1)$ is nucleon density of the projectile, $\rho_2(r_2)$ is the nucleon density of the target and $V(r_{12})$ is the nucleon-nucleon interaction potential with M3Y. Density distribution of ^{10}Be has been used as gaussian density in the following form [20]

$$\rho(r) = \rho_0 \exp(-\beta r^2) \quad (13)$$

where $\rho_0 = 0.0992 \text{ fm}^{-3}$ and $\beta = 0.424 \text{ fm}^{-2}$. Density distribution of ^{120}Sn has been taken from the Ref. [21].

3. Results and Discussion

We investigated the ESCS of ^{11}Be projectile from ^{120}Sn target at 32 MeV by using various potentials within the framework of CDCC model. Since the real part of core (^{10}Be) – target (^{120}Sn) nuclear potential is more effective in $^{11}\text{Be} + ^{120}\text{Sn}$ interaction, we calculated the ESCS for different potentials of $^{10}\text{Be} - ^{120}\text{Sn}$ system. For this, we first used eight type potentials such as Prox

77, Prox 2003-I, Prox 2003-II, Prox 2003-III, Prox 2010, BW 91, AW 95, and CW 76. The changes with r (fm) of the real potentials were shown in Figure 1. The imaginary potential was taken in the Woods-Saxon shape for all the theoretical calculations. The parameters of the imaginary potential were selected as free parameters to provide consistent with the experimental results, and were listed in Table 2.

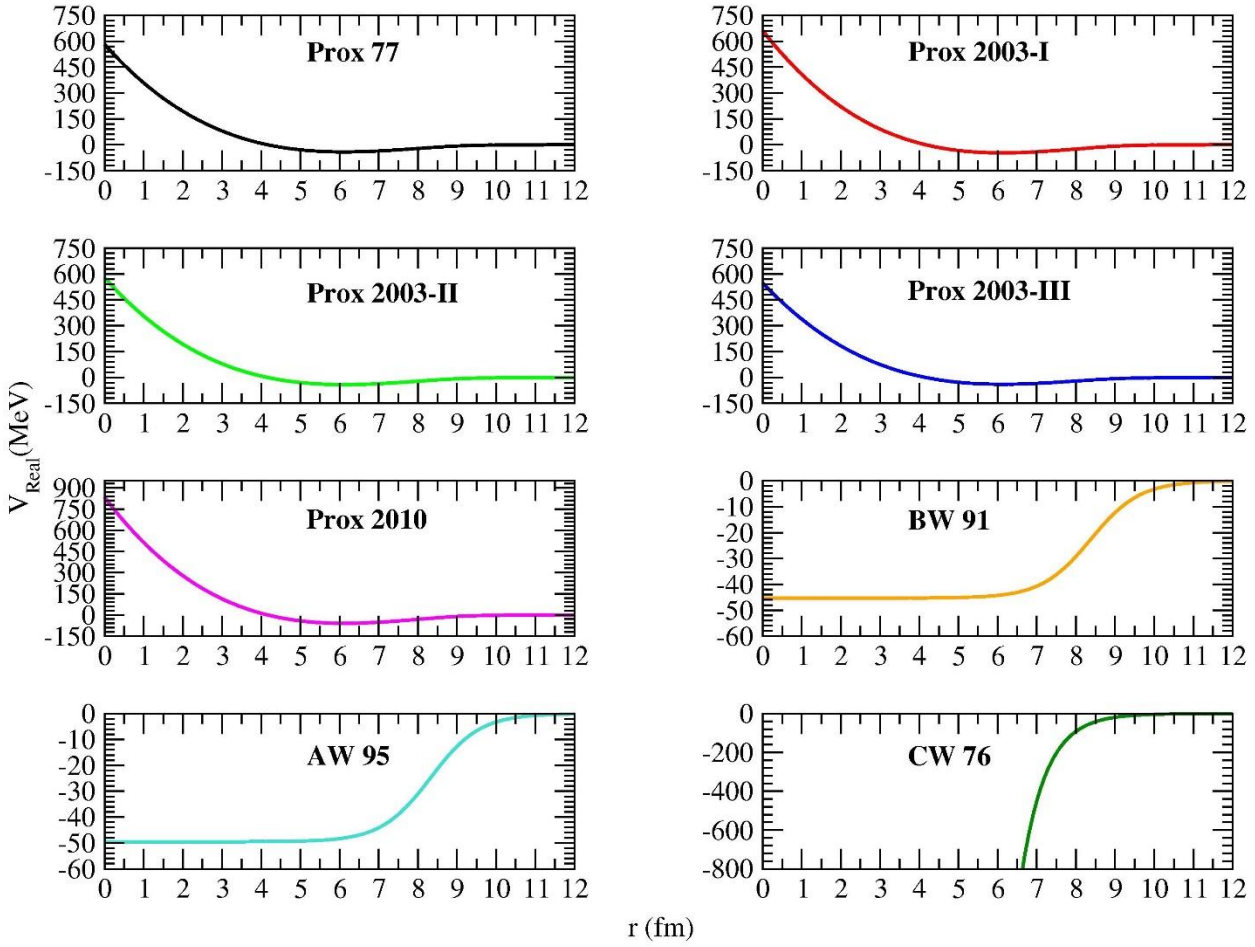


Figure 1. The changes with r (fm) of Prox 77, Prox 2003-I, Prox 2003-II, Prox 2003-III, Prox 2010, BW 91, AW 95 and CW 76 for $^{10}\text{Be} + ^{120}\text{Sn}$ system.

Table 2. Parameters of the core-target imaginary potential for the potentials.

Potential Type	W_0 (MeV)	r_w (fm)	a_w (fm)	χ^2
Prox 77	55	1.39	0.850	0.0495
Prox 2003-I	55	1.39	0.850	0.0661
Prox 2003-II	55	1.39	0.850	0.0661
Prox 2003-III	55	1.39	0.850	0.0661
Prox 2010	55	1.39	0.850	0.0661
BW 91	20	1.39	0.900	0.0656
AW 95	20	1.39	0.900	0.0657
CW 76	20	1.39	0.900	0.0661
Phenomenological	80	1.35	0.900	0.1604
Double Folding	80	1.35	0.857	0.0710

The ESCS calculated for all analyzed potentials are plotted in Figure 2. The theoretical results are coherent with the data at small angles, but are not at large angles.

Additionally, we can see that the result with Prox 77 slightly better than the other potentials.

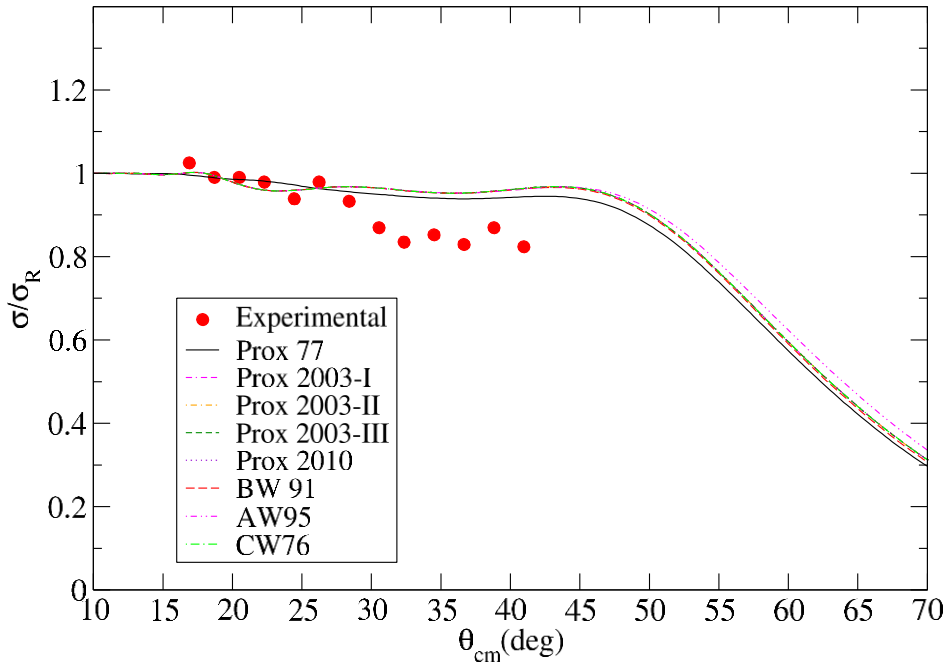


Figure 2. The ESCS of $^{11}\text{Be} + ^{120}\text{Sn}$ system at 32 MeV for Prox 77, 2003-I, 2003-II, 2003-III, 2010, BW 91, AW 95 and CW 76. The experimental data is taken from Ref. [22].

We also compared the results of Prox 77 potential with the results of phenomenological and double folding potentials in Figure 3. We also gave the potential parameters in Table 2. We observed that the result of optical potential is close to the oscillating structure seen at the data. Moreover, we noticed that the optical potential has given closer results to the data while other potentials cannot approach the data at forwards angles.

From this point of view, it can be said that the compatibility of the results of the optical potential with the experimental data is better than the results of both Prox 77 and double folding potential. We think that this is because the variable parameter of the optical potential is higher than the other potentials, and the change of both real and imaginary potentials is more effective.

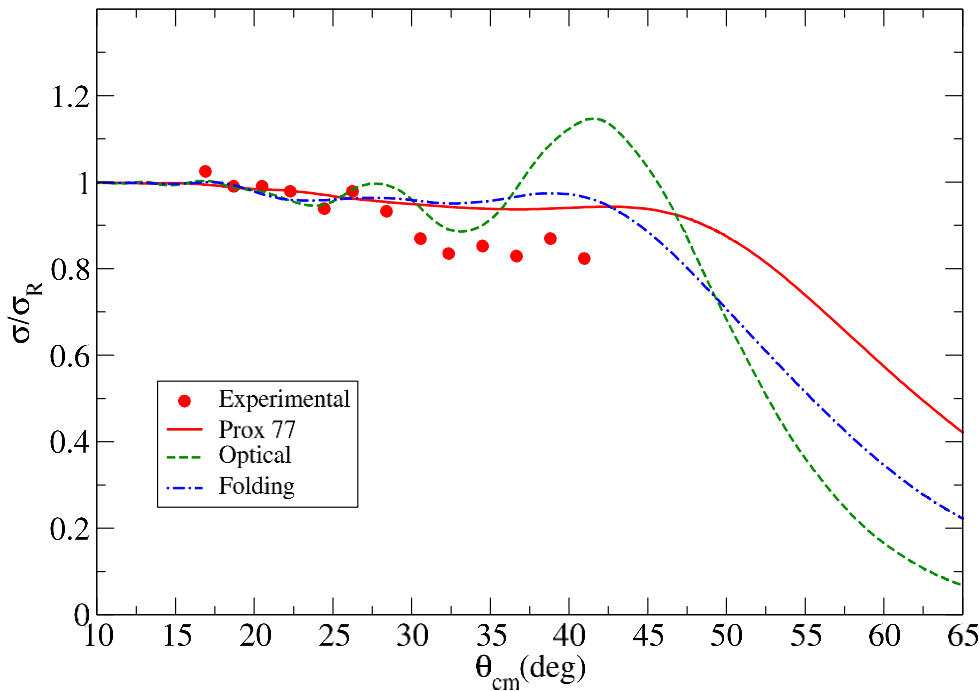


Figure 3. Comparison of the ESCS with Prox 77, phenomenological and double folding potentials of $^{11}\text{Be} + ^{120}\text{Sn}$ system at 32 MeV. The experimental data is taken from Ref. [22].

4. Summary

In this study, we focused on the effect of different nuclear potentials on the CDCC calculations for $^{11}\text{Be} + ^{120}\text{Sn}$ elastic scattering reaction at 32 MeV. We used eight different potentials for the real potential. We compared our results with the data. Then, we compared the results of Prox 77 potential with the results of phenomenological and double Folding potentials. We noticed that the optical potential gives better result than Prox 77 and double folding potentials. Consequently, Prox 77 potential can be suggested as alternative potential compared to other proximity potentials in CDCC analysis of nuclear interactions.

Conflicts of interest

The authors state that there is no financial interests or non financial interests in the subject matter or materials discussed in the manuscript.

References

- [1] Gharaei R., Zanganeh V., Wang N., Systematic study of proximity potentials for heavy-ion fusion cross sections, *Nucl. Phys. A*, 979 (2018) 237-250.
- [2] Bass R., Nucleus-Nucleus potential deduced from experimental fusion cross sections, *Phys. Rev. Lett.*, 39 (1977) 265.
- [3] Reisdorf W., Heavy-ion reactions close to the Coulomb barrier, *J. Phys. G Nucl. Part. Phys.*, 20 (1994) 1297.
- [4] Winther A., Dissipation, polarization and fluctuation in grazing heavy-ion collisions and the boundary to the chaotic regime, *Nucl. Phys. A*, 594 (1995) 203.
- [5] Aygün M., Comparative analysis of proximity potentials to describe scattering of ^{13}C projectile off ^{12}C , ^{16}O , ^{28}Si and ^{208}Pb nuclei, *Revista Mex. De fisica. E*, 64 (2018) 149-153.
- [6] Aygun M., Alternative Potentials Analyzing the Scattering Cross Sections of 7,9,10,11,12,14Be Isotopes from a 12C target: Proximity Potentials, *J. Korean Phy. Soc.*, 73 (2018) 1-8.
- [7] Aygun M., The application of some nuclear potentials for quasielastic scattering data of the $^{11}\text{Li} + ^{28}\text{Si}$ reaction and its consequences, *Turk. J. Phys.*, 42 (2018) 302-311.
- [8] Aygün M., A comparison of proximity potentials in the analysis of heavy-ion elastic cross sections, *Ukr. J. Phys.*, 63 (2018) 10.
- [9] Takashina, M., Sakuragi, Y., Iseri, Y., Effect of halo structure on $^{11}\text{Be} + ^{12}\text{C}$ elastic scattering, *Eur. Phys. J. A*, 25 (2005) 273.
- [10] Rusek K., Martel I., Sánchez-Benítez A.M., Acosta L., ^{10}Be yield from $^{11}\text{Be} + ^{120}\text{Sn}$ interaction at the Coulomb barrier, *Acta Phys. Pol. B*, 43 (2012) 2.
- [11] Deltuva A., Moro A. M., Cravo E., Nunes F. M., A. C. Fonseca, Three-body description of direct nuclear reactions: Comparison with the continuum discretized coupled channels method, *Phys. Rev. C*, 76 (2007) 064602.
- [12] Di Pietro, A., Randisi, G., Scuderi, V., Acosta, L., Amorini, F., Borge, M. J. G., Figuera, P., Fisichella, M., Fraile, L. M., Gomes-Camacho, J. et al., Elastic scattering and reaction mechanisms of the halo nucleus ^{11}Be around the coulomb barrier, *Phys. Rev. Lett.* 105 (2010) 022701.
- [13] Summers N. C. and Nunes F.M., Core excitation in the elastic scattering and breakup of ^{11}Be on protons, *Phys. Rev. C*, 76 (2007) 014611.
- [14] Sparenberg J.M., Baye D., Imanishi B., Coupled-reaction-channel calculations of the $^{16}\text{O}+^{17}\text{O}$ and $^{16}\text{O}+^{17}\text{F}$ charge-symmetric systems, *Phys. Rev. C*, 61 (2000) 054610.
- [15] Becchetti F.D., Greenlees G.W., Nucleon-Nucleus optical-model parameters, $A>40, E<50\text{MeV}$, *Phys. Rev.*, 182 (1969) 1190-1209.
- [16] Zhang G.L., Yao Y.J., Guo M.F., Pan M., Zhang G. X., Liu X.X., Comparative studies for different proximity potentials applied to large cluster radioactivity of nuclei, *Nucl. Phys. A*, 951 (2016) 86–96.
- [17] Dutt I. and Puri R. K., Comparison of different proximity potentials for asymmetric colliding nuclei, *Phys. Rev. C*, 81 (2010) 064609.
- [18] Blocki J., Randrup J. J., Swiatecki W.J., Tsang C.F., Proximity forces, *Ann. Phys.*, 105(2) (1977).

- [19] Christensen P.R. and Winther A., The evidence of the ion-ion potentials from heavy ion elastic scattering, *Phys.Lett. B*, 65 (1976) 19.
- [20] Ibraheem A. A., Analysis of deuteron-nucleus scattering using sao paulo potential, *Braz. J. Phys.*, 46 (2016) 746–753.
- [21] Ficenec J. R., Fajardo L. A., Trowe W. P. R, and Sick I., Elastic electron-tin scattering, *Phys. Lett. B*, 42 (1972) 213.
- [22] Acosta L., Alvarez M.A.G., Andres M.V., Borge M.J.G., Cortes M, J.M. Espino, Galaviz D., Gomez-Camacho J, Maira A, Martel I, Moro A.M., Mukha I., Perez-Bernal F., Reillo E., Rodriguez D., Rusek K. , Sanchez-Benitez A.M., and Tengblad O., Signature of a strong coupling with the continuum in $^{11}\text{Be} + ^{120}\text{Sn}$ scattering at the Coulomb barrier, *Eur. Phys. J. A*, 42 (2009) 461–464.